SCIENCE CHINA
Information Sciences

• RESEARCH PAPER •

April 2021, Vol. 64 142401:1–142401:10
https://doi.org/10.1007/s11432-020-2974-9

Resolution limit of mode-localised sensors

Zhao ZHANG & Honglong CHANG*

Ministry of Education Key Laboratory of Micro/Nano Systems for Aerospace, School of Mechanical Engineering, Northwestern Polytechnical University, Xi'an 710072, China

Received 22 February 2020/Revised 7 May 2020/Accepted 2 July 2020/Published online 25 November 2020

Abstract In recent years, the mode localisation phenomenon of weakly coupled resonators has been successfully utilised to improve the sensitivity of microelectromechanical system (MEMS) sensors. However, controversy remians about the resolution limits of mode-localised sensors. This paper asks two questions of the community: what are the resolution limits of the mode-localised sensors, and can the resolution improvement be obtained using mode-localised sensing? To answer these questions, we report a series of resolution models of mode-localised sensors. We conclude that mode-localised sensing can realise a higher measuring resolution by orders of magnitude when more than three resonators are weakly coupled, and this will lay the theoretical foundation for a breakthrough for the MEMS sensors industry.

Keywords MEMS, mode-localised sensors, resolution limit, 2-degree-of-freedom, higher degree-of-freedom

Citation Zhang Z, Chang H L. Resolution limit of mode-localised sensors. Sci China Inf Sci, 2021, 64(4): 142401, https://doi.org/10.1007/s11432-020-2974-9

1 Introduction

Microelectromechanical system (MEMS) sensors have given birth to a large industry and there are billions of MEMS units sold every year [1]. Microelectromechanical system sensors have been well developed and widely used in consumer electronics, as well as automobile and healthcare fields. Although the MEMS industry is booming, it appears that several kinds of MEMS sensors have reached their fundamental accuracy limit [2, 3]. It is difficult to improve the practical resolution limit further as the fabrication process and signal conditioning capabilities have reached a bottleneck state. For example, the etching aspect ratio has been improved to 40:1 under the current deep reactive ion etching process to improve the capacitance [4]. The vacuum packaging level has been increased to a few pascals to increase the quality factor to the millions [5]. These process technologies already operate at a high level, and further improvement is difficult to achieve. Nevertheless, to make such improvements to performance, a variety of novel methods have been proposed, such as using two-dimensional (2D) materials [6] and new principles [7]. However, often, these attempts are not fully compatible with current MEMS foundry, which has already existed as a large industry for some time.

Among these attempts, mode-localised sensors in which two or more resonators are weakly coupled to improve the sensitivity of MEMS sensors [8–11] are fully compatible with current MEMS foundry. Under the mode-localised sensing paradigm, the frequently used output metric is the amplitude ratio (AR) of two resonators. Owing to the mode localisation phenomenon of weakly coupled resonators (WCRs) [12, 13], the sensitivity of the AR output metric is at least two or three orders of magnitude higher than that of the resonant frequency, which has been theoretically and experimentally demonstrated by various types of WCRs-based resonant sensors [14]. Nevertheless, to what extent the mode-localised sensing paradigm influences the ultimate resolution remains unknown. In 2018, this idea even was regarded as the most important fundamental research question in this field [15].

For mode-localised sensors, thermomechanical noise is the most important factor in determining the lowest detection limit of sensors [16]. This noise is usually caused by Brownian motion around the resonators in an equilibrium position and is strongly dependent on the temperature and damping of

* Corresponding author (email: changhl@nwpu.edu.cn)

© Science China Press and Springer-Verlag GmbH Germany, part of Springer Nature 2020 info.scichina.com link.springer.com

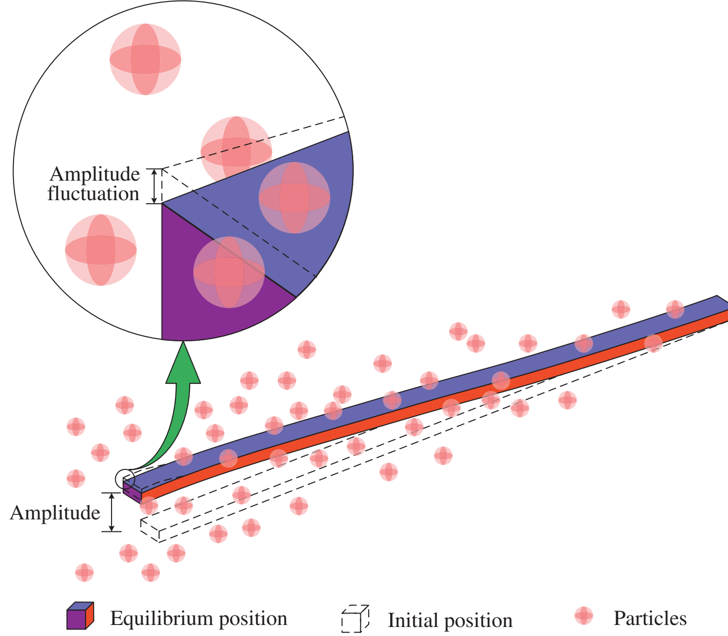

Figure 1 (Color online) Schematic diagram of thermomechanical noise mechanism of a resonator.

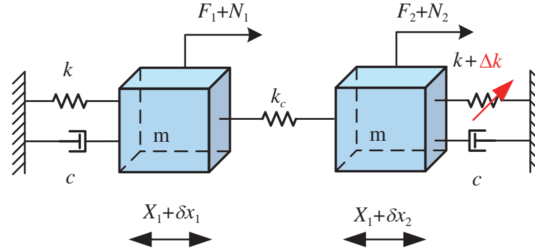

Figure 2 (Color online) Schematic diagram of 2-DoF WCRs.

the system [17]. Owing to molecular motion, damping around the structure disturbs the resonators' motion and provides a path to dissipate energy in the resonant system. Meanwhile, the dissipation has fluctuations acting on the resonators. Figure 1 indicates that the thermomechanical noise causes particles to move around the resonator, leading to the amplitude fluctuation based on the amplitude of the equilibrium position. Therefore, it is fair to conclude that thermomechanical noise determines the resolution limit of mode-localised sensors.

The beam in Figure 1 indicates two positions: the initial position and the equilibrium position. When a driving force has an angular frequency that is the same as the natural frequency of the beam, the beam is resonant, and its equilibrium position shows the mode shape and amplitude compared with its initial position. Particles around the beam represent the damping, which is also the reason for thermomechanical noise. The particles will lead to an amplitude fluctuation at its equilibrium position. In this paper, we analyse how thermomechanical noise determines the ultimate resolution of mode-localised sensors. According to the Equipartition theorem, the Nyquist relation and Laplace transformation [18, 19] of differential equations of a 2-degree-of-freedom (2-DoF) mode-localised resonant system, we report our resolution model of the mode-localised sensors. Based on the model, we have uncovered some interesting findings with regard to the mode-localised sensors that reveal their resolution limit.

2 Results and discussion

2.1 Theoretical resolution limit of 2-DoF mode-localised sensors

In Figure 2, each resonator is simplified as a mass-spring-damping system with the same parameters of mass (m), stiffness (resonator stiffness k and coupling spring stiffness k_c) and damping (c). F_i is

the external driving force acting on the ith resonator. N_i is the equivalent fluctuating force caused by thermomechanical noise. X_i is the displacement of the ith resonator. δx_i is the fluctuation displacement of the ith resonator, and Δk is stiffness perturbation.

First, we analyse the resolution limit for the 2-DoF mode-localised sensors when the resonators are identical and weakly coupled, as seen in Figure 2. We then define κ as the coupling factor of WCRs, and this is calculated by the stiffness ratio between the coupling spring and resonator: $\kappa = k_c/k$.

The resonant system is symmetrical and each resonator has the same motion amplitude without perturbation, and the vibration energy distributes uniformly in each resonator. In the presence of stiffness perturbation, a drastic variation of amplitudes of resonators caused by mode localisation can be observed [20]. The first model on the resolution of the mode-localised sensing based on the AR output metric was established by Seshia et al. [21] from the University of Cambridge. In the model, the minimum resolvable modeshape variation is expressed as [21]

$$\Delta \left|\frac{x_2}{x_1}\right|_{\min} \Big/ \left|\frac{x_2^0}{x_1^0}\right| = \Delta \left(\frac{x_2^{\text{noise}}}{x_2^0} \pm \frac{x_1^{\text{noise}}}{x_1^0}\right), \tag{1}$$

where $\Delta|x_2/x_1|_{\min}$ is the minimum detectable AR change; $|x_2^0/x_1^0|$ is the theoretical AR without noise fluctuations; x_i^{noise} corresponds to the amplitude fluctuations of each resonator, which is determined by the thermomechanical noises; and x_i^0 represents the amplitude of each resonator without fluctuations theoretically.

For mode-localised sensors, the output signal is in voltage form. Thus, the resolution limit can be defined as the minimum detectable signal divided by sensitivity of sensors and then multiplied by the frequency bandwidth around the resonant frequency [22]:

$$R_{AR} = \frac{A_N}{A_U}\frac{\Delta f^{1/2}}{S} = \left(\frac{x_2^{\text{noise}}}{x_2^0} \pm \frac{x_1^{\text{noise}}}{x_1^0}\right)\frac{\Delta f^{1/2}}{S}, \tag{2}$$

where A_N and A_U represent the amplitudes caused by thermomechanical noise and driving force, respectively, S is the sensitivity of mode-localised sensors and Δf is the frequency bandwidth around the resonant frequency.

Based on (2), we will deduce the resolution model of the mode-localised sensors. Therefore, we need to calculate the amplitudes A_N and A_U first.

2.2 Amplitudes without fluctuations

According to Figure 2, we calculate the amplitudes of each resonator, X_i (X_i equals to x_i^0 in (2)), based on the Laplace transformation in the absence of fluctuations ($N_1 = N_2 = 0, \delta x_1 = \delta x_2 = 0$). The motions of the 2-DoF resonant system can be described by two differential equations:

$$\begin{cases} m\ddot{X}_1 + c\dot{X}_1 + kX_1 = k_c(X_2 - X_1) + F_1, \\ m\ddot{X}_2 + c\dot{X}_2 + (k + \Delta k)X_2 = k_c(X_1 - X_2) + F_2, \end{cases} \tag{3}$$

where X_i is displacement of the ith resonator and F_i is the external driving force acting on the ith resonator. Then, we can perform a Laplace transformation and get the amplitude information of each resonator:

$$\begin{cases} X_1 = \dfrac{(-\frac{\omega^2}{\omega_0^2} + \mathrm{j}\frac{\omega}{Q\omega_0} + 1 + \kappa + \epsilon)F_1 + \kappa F_2}{Bm\omega_0^2}, \\ X_2 = \dfrac{\kappa F_1 + (-\frac{\omega^2}{\omega_0^2} + \mathrm{j}\frac{\omega}{Q\omega_0} + 1 + \kappa)F_2}{Bm\omega_0^2}, \end{cases} \tag{4}$$

where ω is the angular frequency of driving force F_i and ω_0 is the natural frequency of the resonator: $\omega_0 = \sqrt{k/m}$; j is an imaginary unit; ϵ is the ratio between stiffness perturbation Δk and the stiffness of resonator k: $\epsilon = \Delta k/k$; and Q is the quality factor, which can be expressed as $Q = m\omega_0/c$. B is a long polynomial produced during computing the inverse matrix [23].

When $F_1 = F$ and $F_2 = 0$, we can get X_i, AR and sensitivity (S) of the system:

$$\begin{cases} X_1 = \dfrac{(-\frac{\omega^2}{\omega_0^2} + \mathrm{j}\frac{\omega}{Q\omega_0} + 1 + \kappa + \epsilon)F}{Bm\omega_0^2}, \\ X_2 = \dfrac{\kappa F}{Bm\omega_0^2}, \end{cases} \tag{5}$$

$$AR = \frac{X_1}{X_2} = \frac{\sqrt{(1 + \kappa + \epsilon - \frac{\omega^2}{\omega_0^2})^2 + \frac{\omega^2}{Q^2\omega_0^2}}}{\kappa}, \tag{6}$$

$$S = \frac{\partial(X_1/X_2)}{\partial\epsilon} = \frac{1 + \kappa + \epsilon - \frac{\omega^2}{\omega_0^2}}{\kappa\sqrt{(1 + \kappa + \epsilon - \frac{\omega^2}{\omega_0^2})^2 + \frac{\omega^2}{Q^2\omega_0^2}}}. \tag{7}$$

In this way, we have calculated the displacement of X_i, which is also the A_U as defined in (2). Then we consider how to express the A_N when there is thermomechanical noise in the resonant system.

2.3 Amplitudes caused by thermomechanical noise

Thermomechanical noise correlates to the Brownian motion of particles and is strongly related to the temperature and damping surrounding the structure. The damping dissipates the energy of the resonators and, at the same time, adds a component of fluctuation to the resonant system [16]. Thus, it is reasonable to use a fluctuation force N_i to represent the thermomechanical noise in the system. Then, we can use differential equations of motion to calculate the response amplitudes with excitation N_i in the frequency domain. Meanwhile, it is acceptable to use the fluctuating force N_i to represent the influence of thermomechanical noise in the system using Laplace transformation to transform the equations of motion into the frequency domain [24]. Therefore, in this paper and for the first time, we use the fluctuation force N_i in the differential equations of motion to calculate amplitudes with thermomechanical noise excitation of mode-localised sensors based on the AR output metric.

According to Figure 2, the motion of the 2-DoF resonant system with fluctuating force N_i caused by thermomechanical noise can be expressed as

$$\begin{cases} m\delta\ddot{x}_1 + c\delta\dot{x}_1 + k\delta x_1 = k_c(\delta x_2 - \delta x_1) + N_1, \\ m\delta\ddot{x}_2 + c\delta\dot{x}_2 + (k + \Delta k)\delta x_2 = k_c(\delta x_1 - \delta x_2) + N_2, \end{cases} \tag{8}$$

where δx_i (δx_i equals to x_i^{noise} in (2)) is the fluctuation displacement of ith resonator, which is also the A_N as defined in (2). Then we can get the expression of it using Laplace transformation:

$$\begin{cases} \delta x_1 = \dfrac{(-\frac{\omega^2}{\omega_0^2} + \mathrm{j}\frac{\omega}{Q\omega_0} + 1 + \kappa + \epsilon)N_1 + \kappa N_2}{Bm\omega_0^2}, \\ \delta x_2 = \dfrac{\kappa N_1 + (-\frac{\omega^2}{\omega_0^2} + \mathrm{j}\frac{\omega}{Q\omega_0} + 1 + \kappa)N_2}{Bm\omega_0^2}. \end{cases} \tag{9}$$

2.4 Ultimate resolution model of a 2-DoF mode-localised sensor

Once we find a way to express X_i and δx_i, we can deduce an explicit equation of thermomechanical noise influencing the resonant system. According to (1) and (2) for a 2-DoF mode-localised sensor, we find

$$\frac{A_N}{A_U} = \frac{\delta x_1}{X_1} \pm \frac{\delta x_2}{X_2} = \frac{(-\frac{\omega^2}{\omega_0^2} + \mathrm{j}\frac{\omega}{Q\omega_0} + 1 + \kappa + +\epsilon)N_1 + \kappa N_2}{(-\frac{\omega^2}{\omega_0^2} + \mathrm{j}\frac{\omega}{Q\omega_0} + 1 + \kappa + +\epsilon)F_1 + \kappa F_2} \pm \frac{\kappa N_1 + (-\frac{\omega^2}{\omega_0^2} + \mathrm{j}\frac{\omega}{Q\omega_0} + 1 + \kappa)N_2}{\kappa F_1 + (-\frac{\omega^2}{\omega_0^2} + \mathrm{j}\frac{\omega}{Q\omega_0} + 1 + \kappa)F_2}. \tag{10}$$

Mode-localised sensors are driven at resonant frequency. There are two resonant frequencies and two resonant modes of a 2-DoF resonant system. The frequencies of the first mode (in-phase mode) and the second mode (out-of-phase mode) are, respectively,

$$\begin{cases} \omega_1 = \sqrt{\dfrac{k}{m}}, \\ \omega_2 = \sqrt{\dfrac{k + 2k_c}{m}}. \end{cases} \tag{11}$$

In particular, when $\epsilon = 0$ and ω in (9) equals to the resonant frequency ω_1, which is the resonant frequency of the first mode for mode-localised sensors. $\epsilon = 0$ means there is no disturbance from outside, and we use this condition which is the same as conditions in [14, 25] to establish the resolution model, and then we can get

$$\begin{cases} \delta x_1\big|_{\substack{\epsilon=0\\ \omega=\omega_1}} = \dfrac{(\kappa + \mathrm{j}\frac{1}{Q})N_1 + \kappa N_2}{Bm\omega_0^2}, \\ \delta x_2\big|_{\substack{\epsilon=0\\ \omega=\omega_1}} = \dfrac{\kappa N_1 + (\kappa + \mathrm{j}\frac{1}{Q})N_2}{Bm\omega_0^2}, \\ X_1\big|_{\substack{\epsilon=0\\ \omega=\omega_1}} \approx X_2\big|_{\substack{\epsilon=0\\ \omega=\omega_1}} = \dfrac{\kappa F}{Bm\omega_0^2}, \\ B\big|_{\substack{\epsilon=0\\ \omega=\omega_1}} \approx \dfrac{2\kappa}{Q}, \end{cases} \tag{12}$$

$$\left.\frac{A_N}{A_U}\right|_{\substack{\epsilon=0\\ \omega=\omega_1}} = \frac{\delta x_1}{X_1} + \frac{\delta x_2}{X_2} \approx 2\left(\frac{N_1}{F_1} + \frac{N_2}{F_2}\right). \tag{13}$$

The sensitivity of the 2-DoF resonant system can be calculated according to (6):

$$S = \left.\frac{\partial(X_1/X_2)}{\partial \epsilon}\right|_{\substack{\epsilon=0\\ \omega=\omega_1}} \approx \frac{1}{\kappa}. \tag{14}$$

Finally, we deduce the resolution limit for the 2-DoF mode-localised system based on (2), (13) and (14):

$$R_{AR} = 2\kappa\left(\frac{N_1}{F_1} + \frac{N_2}{F_2}\right)\Delta f^{1/2}, \tag{15}$$

where N_i mainly depends on temperature and damping. For the two resonators in the system, they oscillate under the same circumstance, almost with the same temperature and damping. Thus, we can get

$$N_1 \approx N_2 = N = \sqrt{4k_BTc}. \tag{16}$$

Then, according to (7) in [21], Eq. (15) can be re-expressed as

$$R_{AR} \approx 2\sqrt{2}\kappa\frac{N}{F}\Delta f^{1/2} = 2\sqrt{2}\kappa\frac{\sqrt{4k_BTc\Delta f}}{F}. \tag{17}$$

From (17), we notice that R_{AR} is proportional to the coupling factor κ, which means we can improve the resolution limit by decreasing the ratio between the stiffness of the coupling spring and the resonator. Compared with the resolution model in [21], the explicit expression reveals that the resolution limit in the weakly coupled resonant system depends on the ratio of A_N/A_U, and the ultimate resolution of mode-localised sensors can be improved by decreasing the coupling factor κ.

$$\begin{cases} \delta x_1 + \delta x_2 = Q(N_1 + N_2)\dfrac{1}{m\omega_0^2}, \\ \delta x_1 - \delta x_2 = \dfrac{N_1 - N_2}{2\kappa}\dfrac{1}{m\omega_0^2}. \end{cases} \tag{18}$$

Compared with the resolution model [25] in which the resolution limit is independent of κ, as illustrated in Table 1, our model reveals that the ultimate resolution of mode-localised sensors can be improved by decreasing the coupling factor κ. We can see from (18) that $\delta x_1 + \delta x_2$ and $\delta x_1 - \delta x_2$ are not the same as the minus sign in $\delta x_1 - \delta x_2$ and has influences on other items except N_1 and N_2. This accounts for our different resolution model in comparison with [25] in which $\delta x_1 - \delta x_2$ is regarded as a whole.

2.5 Theoretical resolution limit of higher DoF mode-localised sensors

Higher DoF mode-localised sensors, like 3-DoF [26] and 4-DoF [27], are demonstrated in Figure 3. Each resonator is simplified as a mass-spring-damping system with the same parameters of mass (m), stiffness (resonator stiffness k and coupling spring stiffness k_c) and damping (c). F_i is the external driving force

Table 1 Comparison of resolution limit model of 2-DoF WCRs

	Resolution limit model
This model	$R_{AR} \approx 2\sqrt{2}\kappa \frac{N}{F}\Delta f^{1/2} = 2\sqrt{2}\kappa \frac{\sqrt{4k_BTc\Delta f}}{F}$
A. Seshia [21]	$R_{AR} \approx 8\kappa\sqrt{\frac{E_{\rm th}\Delta f}{2E_cQ\omega_{\rm eff}}} = 8\kappa\sqrt{\frac{k_BTC_c^{\rm eff}\Delta f}{(m_r^{\rm eff})^2(\omega_{\rm eff})^4(X_r^0)^2}}$
Jérôme Juillard [24]	$R_{AR} = \frac{2N}{QF}\Delta f^{1/2}$

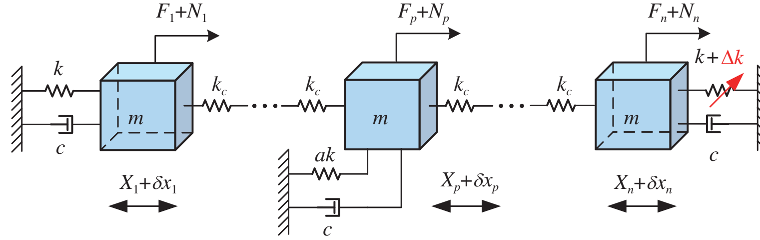

Figure 3 (Color online) Schematic diagram of multi-DoF WCRs.

acting on the ith resonator. N_i is the equivalent fluctuating force caused by thermomechanical noise. X_i is the displacement of the ith resonator. δx_i is the fluctuation displacement of the ith resonator. And Δk is the stiffness perturbation. The two outer resonators contain the same factors. Moreover, the stiffness of the resonators in the middle of the resonant system is larger than that of the outer resonators. The ratio between the stiffness of the middle resonators and the stiffness of the outer resonators is a.

When we choose the AR of outer resonators as the output metric, we can use the same method to deduce the resolution limit of a multi-DoF with (2). Then we can get the differential equations of the resonant system to calculate X_i and δx_i in Figure 3:

$$\begin{cases} m\ddot{X}_1 + c\dot{X}_1 + kX_1 = k_c(X_2 - X_1) + F_1, \\ \quad\vdots \\ m\ddot{X}_p + c\dot{X}_p + akX_p = k_c(X_{p-1} + X_{p+1} - 2X_p) + F_p, \\ \quad\vdots \\ m\ddot{X}_n + c\dot{X}_n + (k+\Delta k)X_n = k_c(X_{n-1} - X_n) + F_n, \end{cases} \tag{19}$$

$$\begin{cases} m\ddot{\delta x}_1 + c\dot{\delta x}_1 + k\delta x_1 = k_c(\delta x_2 - \delta x_1) + N_1, \\ \quad\vdots \\ m\ddot{\delta x}_p + c\dot{\delta x}_p + ak\delta x_p = k_c(\delta x_{p-1} + \delta x_{p+1} - 2\delta x_p) + N_p, \\ \quad\vdots \\ m\ddot{\delta x}_n + c\dot{\delta x}_n + (k+\Delta k)\delta x_n = k_c(\delta x_{n-1} - \delta x_n) + N_n, \end{cases} \tag{20}$$

where p is a resonator in the middle of resonant system. We just need the amplitude ratio of the two outer resonators, which means the way to calculate A_N and A_U is the same as before. Then we get the expressions of A_N and A_U. B' is a complicated polynomial produced during computing the inverse matrix:

$$\begin{cases} X_1 = \dfrac{C_{11}F_1 + \cdots + C_{1n}F_n}{B'm\omega_0^2}, \\ X_n = \dfrac{C_{n1}F_1 + \cdots + C_{nn}F_n}{B'm\omega_0^2}, \end{cases} \tag{21}$$

$$\begin{cases} \delta x_1 = \dfrac{C_{11}N_1 + \cdots + C_{1n}N_n}{B'm\omega_0^2}, \\ \delta x_n = \dfrac{C_{n1}N_1 + \cdots + C_{nn}N_n}{B'm\omega_0^2}, \end{cases} \tag{22}$$

Table 2 Comparison of resolution limit model using frequency and AR output metrics

		Resolution limit model
Frequency output metric		$\frac{1}{Q}\frac{N}{F}\Delta f^{1/2}$
AR output metric	2-DoF	$2\sqrt{2}\kappa\frac{N}{F}\Delta f^{1/2}$
	3-DoF	$\frac{2\sqrt{2}\kappa^2}{a-1}\frac{N}{F}\Delta f^{1/2}$
	4-DoF	$\frac{2\sqrt{2}\kappa^3}{(a-1)^2}\frac{N}{F}\Delta f^{1/2}$

$$\frac{A_N}{A_U}=\frac{\delta x_1}{X_1}\pm\frac{\delta x_n}{X_n}=\frac{C_{11}N_1+\cdots+C_{1n}N_n}{C_{11}F_1+\cdots+C_{1n}F_n}\pm\frac{C_{n1}N_1+\cdots+C_{nn}N_n}{C_{n1}F_1+\cdots+C_{nn}F_n}. \tag{23}$$

Because the sensitivity is increased with increasing DoF [26–28], the resolution limit for a higher DoF resonant system will improve. According to our calculation, the sensitivity of a 3-DoF system is related to κ^2 and the sensitivity of a 4-DoF system is related to κ^3:

$$R_{\text{3-Dof}}=\left.\frac{\delta(X_1/X_3)}{\delta\epsilon}\right|_{\substack{\epsilon=0\\ \omega/\omega_0=1}}\approx\frac{a+\kappa-1}{\kappa^2}\approx\frac{a-1}{\kappa^2}, \tag{24}$$

$$R_{\text{4-Dof}}=\left.\frac{\delta(X_1/X_3)}{\delta\epsilon}\right|_{\substack{\epsilon=0\\ \omega/\omega_0=1}}\approx\frac{(a-2)^2-\kappa^2}{\kappa^3}\approx\frac{(a-2)^2}{\kappa^3}. \tag{25}$$

Thus, the resolution limit for 3-DoF and 4-DoF resonant systems may be expressed, respectively, as

$$R_{\text{AR,3-Dof}}\approx\frac{2\sqrt{2}\kappa^2}{(a-1)}\frac{N}{F}\Delta f^{1/2}=\frac{2\sqrt{2}\kappa^2}{(a-1)}\frac{\sqrt{4k_BT_c\Delta f}}{F}, \tag{26}$$

$$R_{\text{AR,4-Dof}}\approx\frac{2\sqrt{2}\kappa^3}{(a-2)^2}\frac{N}{F}\Delta f^{1/2}=\frac{2\sqrt{2}\kappa^3}{(a-2)^2}\frac{\sqrt{4k_BT_c\Delta f}}{F}. \tag{27}$$

The resolution for a single resonator using frequency as the readout metric can be expressed as [29]

$$R_{\omega_0}=\frac{1}{Q}\frac{N}{F}\Delta f^{1/2}, \tag{28}$$

where Q is the quality factor; κ is the coupling factor; a is ratio between the stiffness of the middle resonators and the outer resonators and its value is 3 [26].

In Table 2, the resolution limit of the sensors based on the frequency-output metric is proportional to $1/Q$ [29], and the resolution limits based on the AR output metric of 2-DoF, 3-DoF and 4-DoF are proportional to κ, κ^2 and κ^3. It can be seen that the resolution limit of the frequency-output metric has a better resolution than the 2-DoF mode-localised sensors using the AR output metric. The 3-DoF mode-localised sensors using the AR output metric have a better resolution limit than both the 2-DoF and frequency-output sensors, and the 4-DoF sensors indicate the best resolution limit, which is three orders better than 3-DoF. This trend coincides with the experimental data in [11, 23, 28]. It can be seen from the experimental data of mode-localised electrometers that the resolution is improved from 8000 e/$\sqrt{\text{Hz}}$ to 9.21 e/$\sqrt{\text{Hz}}$ (3-DoF) and 0.256 e/$\sqrt{\text{Hz}}$ (4-DoF).

Thus, we draw some important conclusion about mode-localised sensors. First, the resolution limit of mode-localised sensors is always related to the coupling factor. We can improve the resolution limit by decreasing the value of it. Second, for 2-DoF mode-localised sensors, the frequency-output metric has a better resolution limit than the AR-based output metric since $\kappa Q\gg 1$ is necessary for resolving two peaks in the frequency response of two outer resonators [25]. However, we cannot conclude that the frequency-output metric is better than the AR output metric since the resolution limit of the AR output metric can be improved by increasing DoFs in the system. For the AR output metric, the thermomechanical noise, which is determined by the two outer resonators, would maintain the same level no matter how many resonators exist in the WCR system. Meanwhile, the enhancement of the sensitivity of 3-DoF and 4-DoF mode-localised sensors has been proven theoretically and experimentally [26–28]. Thus, the resolution limit, which primarily depends on noise fluctuations, will improve with the increase in the sensitivity.

The final and most important conclusion is that the resolution limit of the high-order (the DoFs $\geqslant 3$) mode-localised sensors using the AR output metric is better than that of the frequency-output metric. Thus, we can answer the question of whether the ultimate resolution can be improved for mode-localised sensors by increasing the resonators in the mode-localised system, and the resolution limit is better than frequency-output metric based on a single resonator. This conclusion also paves the way for further enhancement of the accuracy of the MEMS sensors based on current fabrication facilities.

3 Models and methods

Based on (2), we use the Laplace transformation to calculate the amplitudes of each resonator as well as the amplitude fluctuations caused by thermomechanical noise in the resonant system. The amplitude X_i originates from differential equations of the resonant system in Figure 3. The dynamic equations in (19) can be used to represent a 2-DoF or a higher DoF resonant system. The difference between them is the middle resonators, whose stiffnesses are at least two times that of the outer resonators.

After simplification, we use Laplace transformation and substitute $S = j\omega$ to obtain a new set of equations from (19):

$$\begin{cases} \left(-\frac{\omega^2}{\omega_0^2} + \mathrm{j}\frac{\omega}{\omega_0 Q} + 1 + \kappa\right) X_1 - \kappa X_2 = \frac{F_1}{m\omega_0^2}, \\ \vdots \\ -\kappa X_{p-1} + \left(-\frac{\omega^2}{\omega_0^2} + \mathrm{j}\frac{\omega}{\omega_0 Q} + a + 2\kappa\right) X_p - \kappa X_{p+1} = \frac{F_p}{m\omega_0^2}, \\ \vdots \\ -\kappa X_{n-1} + \left(-\frac{\omega^2}{\omega_0^2} + \mathrm{j}\frac{\omega}{\omega_0 Q} + 1 + \kappa + \epsilon\right) X_n = \frac{F_n}{m\omega_0^2}, \end{cases} \tag{29}$$

where ω_0 is the natural frequency of resonators and equals to $\sqrt{k/m}$; ω is the angular frequency of driving force F_i; j is the imaginary unit; Q is the quality factor; κ is coupling factor, which is a ratio of k_c/k; and ϵ represents stiffness perturbation, which is a ratio of $\Delta k/k$.

Then we transform (29) into matrix form:

$$A \times X = \frac{1}{m\omega_0^2} F = \begin{bmatrix} D_1 & -\kappa & 0 & \cdots & \cdots & \cdots & 0 \\ -\kappa & \ddots & \ddots & \ddots & \cdots & \cdots & \vdots \\ 0 & \ddots & \ddots & -\kappa & \ddots & \cdots & \vdots \\ \vdots & \ddots & -\kappa & D_p & -\kappa & \ddots & \vdots \\ \vdots & \vdots & \ddots & -\kappa & \ddots & \ddots & 0 \\ \vdots & \vdots & \vdots & \ddots & \ddots & \ddots & -\kappa \\ 0 & \cdots & \cdots & \cdots & 0 & -\kappa & D_n \end{bmatrix}^{-1} \begin{bmatrix} X_1 \\ \vdots \\ \vdots \\ X_p \\ \vdots \\ \vdots \\ X_n \end{bmatrix} = \frac{1}{m\omega_0^2} \begin{bmatrix} F_1 \\ \vdots \\ \vdots \\ F_p \\ \vdots \\ \vdots \\ F_n \end{bmatrix}, \tag{30}$$

$$\begin{cases} D_1 = -\frac{\omega^2}{\omega_0^2} + \mathrm{j}\frac{\omega}{\omega_0 Q} + 1 + \kappa, \\ \vdots \\ D_p = -\frac{\omega^2}{\omega_0^2} + \mathrm{j}\frac{\omega}{\omega_0 Q} + a + 2\kappa, \\ \vdots \\ D_n = -\frac{\omega^2}{\omega_0^2} + \mathrm{j}\frac{\omega}{\omega_0 Q} + 1 + \kappa + \epsilon, \end{cases} \tag{31}$$

where D_i is diagonal element of the system matrix A, X represents a column vector of displacements X_i, F represents the column vector of driving forces F_i.

$$\begin{bmatrix} X_1 \\ \vdots \\ \vdots \\ X_p \\ \vdots \\ \vdots \\ X_n \end{bmatrix} = \frac{1}{m\omega_0^2} \begin{bmatrix} D_1 & -\kappa & 0 & \cdots & \cdots & \cdots & 0 \\ -\kappa & \ddots & \ddots & \ddots & \cdots & \cdots & \vdots \\ 0 & \ddots & \ddots & -\kappa & \ddots & \cdots & \vdots \\ \vdots & \ddots & -\kappa & D_p & -\kappa & \ddots & \vdots \\ \vdots & \vdots & \ddots & -\kappa & \ddots & \ddots & 0 \\ \vdots & \vdots & \vdots & \ddots & \ddots & \ddots & -\kappa \\ 0 & \cdots & \cdots & \cdots & 0 & -\kappa & D_n \end{bmatrix}^{-1} \begin{bmatrix} F_1 \\ \vdots \\ \vdots \\ F_p \\ \vdots \\ \vdots \\ F_n \end{bmatrix}. \tag{32}$$

According to the displacements X_i of each resonator, we can get amplitude ratio between the two outer resonators and sensitivity of the resonant system.

The thermomechanical noise acting on the resonant system can be regarded as fluctuating force N_i to represent the influence in the system [24]. Thus, we get the dynamic equations of a 2-DoF equivalent model as shown in Figure 3:

$$\begin{cases} m\delta\ddot{x}_1 + c\delta\dot{x}_1 + k\delta x_1 = k_c(\delta x_2 - \delta x_1) + N_1, \\ \quad\vdots \\ m\delta\ddot{x}_p + c\delta\dot{x}_p + ak\delta x_p = k_c(\delta x_{p-1} + \delta x_{p+1} - 2\delta x_p) + N_p, \\ \quad\vdots \\ m\delta\ddot{x}_n + c\delta\dot{x}_n + (k+\Delta k)\delta x_n = k_c(\delta x_{n-1} - \delta x_n) + N_n, \end{cases} \tag{33}$$

where N_i represents the magnitude of equivalent force of the thermomechanical noise perturbation. Using Laplace transformation to transform the equations of motion into frequency domain [24], so we can get the magnitude of δx_i after the same processes of X_i:

$$\begin{bmatrix} \delta x_1 \\ \vdots \\ \vdots \\ \delta x_p \\ \vdots \\ \vdots \\ \delta x_n \end{bmatrix} = \frac{1}{m\omega_0^2} \begin{bmatrix} D_1 & -\kappa & 0 & \cdots & \cdots & \cdots & 0 \\ -\kappa & \ddots & \ddots & 0 & \cdots & \cdots & \vdots \\ 0 & \ddots & \ddots & -\kappa & 0 & \cdots & \vdots \\ \vdots & 0 & -\kappa & D_p & -\kappa & 0 & \vdots \\ \vdots & \vdots & 0 & -\kappa & \ddots & \ddots & 0 \\ \vdots & \vdots & \vdots & 0 & \ddots & \ddots & -\kappa \\ 0 & \cdots & \cdots & \cdots & 0 & -\kappa & D_n \end{bmatrix}^{-1} \begin{bmatrix} N_1 \\ \vdots \\ \vdots \\ n_p \\ \vdots \\ \vdots \\ N_n \end{bmatrix}. \tag{34}$$

Mode-localised sensors are driven at a resonant frequency. There are at least two resonant frequencies and two resonant modes for a resonant system. We assume the frequencies of the first mode (in-phase mode) is ω_1, and the second mode (out-of-phase mode) is ω_2. So, in particular, when $\epsilon = 0$, $F_1 = F$, the rest of the driving force is equal to zero, and ω in (9) equals the resonant frequency ω_1, which is the resonant frequency of the first mode for mode-localised sensors [25]. Thus, we can attain AR, sensitivity and the resolution limit of 2, 3 and 4-DoF resonant systems.

4 Conclusion

We have theoretically analysed the resolution limits of mode-localised sensors and compared them with the frequency-output metric. Here we conclude that first, the resolution limit of mode-localised sensors is related to the coupling factor κ, and we can improve the resolution limit by decreasing the value of it. Second, for 2-DoF mode-localised sensors, the frequency-output metric has a better resolution limit. However, the resolution limit of AR-based mode-localised sensors can be improved by increasing DoFs

in the resonant system, and the resolution limit of the high-order (the DoFs $\geqslant 3$) mode-localised sensors using the AR output metric is better than that of the frequency-output metric. This finding provides a theoretical foundation for breakthroughs in the MEMS sensors industry.

In the future, the electrical circuitry noise contribution to the resolution should be studied, and a direct experimental verification can be obtained. Furthermore, the resolution limit with or without mode overlapping should be established since it does not exist at the condition to avoid mode overlapping for high-order systems.

Acknowledgements This work was supported by National Key Research and Development Program of China (Grant No. 2018YFB2002600), National Natural Science Foundation of China (Grant No. 51575454), and Fundamental Research Funds for the Central Universities (Grant No. 3102019JC002). The author would like to show grateful acknowledgment to H. Kang and J. Yang for their helpful discussion.

References

1 Patsavellas J, Salonitis K. The carbon footprint of manufacturing digitalization: critical literature review and future research agenda. Procedia CIRP, 2019, 81: 1354–1359
2 Trusov A, Atikyan G, Rozelle D M, et al. Flat is not dead: current and future performance of Si-MEMS Quad Mass Gyro (QMG) system. In: Proceedings of 2014 IEEE/ION Position, Location and Navigation Symposium, Monterey, 2014. 252–258
3 Ramezani M, Ghatge M, Tabrizian R. High-Q silicon fin bulk acoustic resonators for signal processing beyond the UHF. In: Proceedings of 2017 IEEE International Electron Devices Meeting (IEDM), San Francisco, 2017. 1–4
4 Abdolvand R, Amini B V, Ayazi F. Sub-micro-gravity in-plane accelerometers with reduced capacitive gaps and extra seismic mass. J Microelectromech Syst, 2007, 16: 1036–1043
5 Spletzer M, Raman A, Wu A Q, et al. Ultrasensitive mass sensing using mode localization in coupled microcantilevers. Appl Phys Lett, 2006, 88: 254102
6 Novoselov K S, Mishchenko A, Carvalho A, et al. 2D materials and van der Waals heterostructures. Science, 2016, 353: aac9439
7 de Lépinay L M, Pigeau B, Besga B, et al. A universal and ultrasensitive vectorial nanomechanical sensor for imaging 2D force fields. Nat Nanotech, 2017, 12: 156–162
8 Yang J, Zhong J M, Chang H L. A closed-loop mode-localized accelerometer. J Microelectromech Syst, 2018, 27: 210–217
9 Kang H, Yang J, Chang H L. A closed-loop accelerometer based on three degree-of-freedom weakly coupled resonator with self-elimination of feedthrough signal. IEEE Sens J, 2018, 18: 3960–3967
10 Zhao C, Wood G S, Xie J B, et al. A force sensor based on three weakly coupled resonators with ultrahigh sensitivity. Sens Actuat A-Phys, 2015, 232: 151–162
11 Yang J, Kang H, Chang H L. A micro resonant electrometer with 9-electron charge resolution in room temperature. In: Proceedings of 2018 IEEE Micro Electro Mechanical Systems (MEMS), 2018. 67–70
12 Anderson P W. Absence of diffusion in certain random lattices. Phys Rev, 1958, 109: 1492–1505
13 Hodges C H, Woodhouse J. Confinement of vibration by one-dimensional disorder. I: theory of ensemble averaging. J Sound Vib, 1989, 130: 237–251
14 Zhao C, Wood G S, Xie J B, et al. A comparative study of output metrics for an MEMS resonant sensor consisting of three weakly coupled resonators. J Microelectromech Syst, 2016, 25: 626–636
15 Kraft M. Coupled resonators as a new transduction principle for ultraprecise sensors. In: Proceedings of the 19th ITG/GMA-Symposium on Sensors and Measuring Systems, Nuremberg, 2018. 1–4
16 Álvarez M, Tamayo J, Plaza J A, et al. Dimension dependence of the thermomechanical noise of microcantilevers. J Appl Phys, 2006, 99: 024910
17 Gabrielson T B. Mechanical-thermal noise in micromachined acoustic and vibration sensors. IEEE Trans Electron Dev, 1993, 40: 903–909
18 Sears F W, Salinger G L. Thermodynamics, Kinetic Theory, and Statistical Thermodynamics. Reading: Addison-Wesley Publishing Company Press, 1975
19 Kittel C. Elementary Statistical Physics. New York: Dover Publications Pressed, 2004
20 Hodges C H. Confinement of vibration by structural irregularity. J Sound Vib, 1982, 82: 411–424
21 Thiruvenkatanathan P, Woodhouse J, Yan J, et al. Limits to mode-localized sensing using micro- and nanomechanical resonator arrays. J Appl Phys, 2011, 109: 104903
22 Zhang H M, Li B Y, Yuan W Z, et al. An acceleration sensing method based on the mode localization of weakly coupled resonators. J Microelectromech Syst, 2016, 25: 286–296
23 Zhang H M, Huang J, Yuan W Z, et al. A high-sensitivity micromechanical electrometer based on mode localization of two degree-of-freedom weakly coupled resonators. J Microelectromech Syst, 2016, 25: 937–946
24 Saulson P R. Thermal noise in mechanical experiments. Phys Rev D, 1990, 42: 2437–2445
25 Juillard J, Prache P, Ferreira P M, et al. Ultimate limits of differential resonant MEMS sensors based on two coupled linear resonators. IEEE Trans Ultrason Ferroelect Freq Contr, 2018, 65: 2440–2448
26 Zhao C, Wood G S, Xie J B, et al. A three degree-of-freedom weakly coupled resonator sensor with enhanced stiffness sensitivity. J Microelectromech Syst, 2016, 25: 38–51
27 Kang H, Yang J, Zhong J M, et al. A mode-localised accelerometer based on three degree-of-freedom weakly coupled resonator. In: Proceedings of 2017 IEEE SENSORS, Glasgow, 2017. 1–3
28 Kang H, Ruan B, Hao Y C, et al. A micromachined electrometer with room temperature resolution of 0.256 $e/\sqrt{\text{Hz}}$. IEEE Sens J, 2020, 20: 95–101
29 Juillard J, Prache P, Ferreira P M, et al. Impact of output metric on the resolution of mode-localisedlocalised MEMS resonant sensors. In: Proceedings of 2017 Joint Conference of the European Frequency and Time Forum and IEEE International Frequency Control Symposium (EFTF/IFCS), 2017